



ELSEVIER

Applied Mathematical Modelling 22 (1998) 1071–1080

APPLIED
MATHEMATICAL
MODELLING

A numerical model for predicting bubble formation in a 3D fluidized bed

P.J. Witt ^{a,b,*}, J.H. Perry ^{a,b}, M.P. Schwarz ^a^a CSIRO Minerals, Mineral Processing and Metal Production Sector, Box 312, Clayton South Vic. 3169, Australia^b CRC-New Technologies For Power Generation From Low-Rank Coal, Mulgrave, Vic., Australia

Received 1 July 1997; received in revised form 20 April 1998; accepted 20 April 1998

Abstract

Fluidized bed systems have the potential to be widely used in the power generation, mineral processing and chemical industries. One factor limiting their increased use is the lack of adequate design techniques for scaling such systems. A model has been developed for simulating gas–solid fluidized bed plant. The model uses a multiphase Eulerian–Eulerian technique to predict the transient behaviour of fluidized bed systems. The commercial CFD code CFX is used as the computational framework for solving the discretized equations. To overcome the problem of accurate geometrical representation experienced in previous models a body fitted grid system is employed. The model is used to predict isothermal flow in a three-dimensional bubbling fluidized bed. Predictions of the three-dimensional model show bubble formation with gas bubbles or voids preferentially moving along the centre of the bed. Predicted behaviour is qualitatively consistent with experimental observations. © 1998 Elsevier Science Inc. All rights reserved.

Keywords: Fluidized bed; Eulerian–Eulerian; CFD modelling; Multiphase

1. Introduction

Bubbling and circulating fluidized bed systems are becoming an increasingly important technology for the power generation, mineral and chemical processing industries. Benefits in economic, operational and environmental terms can be achieved with fluidized bed technology over more traditional technologies. The complex fluid mechanics in fluidized bed systems poses a significant challenge and a technological risk to plant designers and investors.

Current techniques for scaling fluidized beds rely on either scaling laws based on dimensional analysis or simple empirical correlations. In systems with well-known behaviour these techniques allow changes in operating parameters to be analysed. However where large changes in scale or operating parameters occur such techniques are often inadequate. For single phase flows CFD modelling has proved to be capable of overcoming such problems and often provides significant insights into the understanding of how the flow behaves.

Early CFD models of fluidized bed systems used specially written codes which are usually limited to two dimensional isothermal flows and simple rectangular geometries [1–4]. This paper reports on recent work undertaken to extend the Eulerian–Eulerian model in the commercial CFD

* Corresponding author. Tel.: +61 3 9545 8500; fax: +61 3 9562 8919.

code CFX (formerly CFDS-FLOW3D) [5] to simulate fluidized bed systems. An advantage of using CFX is that its multiblock facility and body fitted coordinates allow more complex geometries to be handled than was possible in earlier models. Also, advanced numerical techniques developed for single phase flows can be adopted more readily for use in multiphase flow problems.

This paper describes the CFD model and demonstrates its use by applying it to predicting bubbles forming in a three-dimensional fluidized bed.

2. Mathematical model

2.1. Multiphase continuum model

Multiphase gas–solid flows can be modelled using either Eulerian–Lagrangian or Eulerian–Eulerian methods. The most widely used Eulerian–Lagrangian method is the particle tracking method where individual particle trajectories are found by solving Newton’s equations of motion with the drag force being found from the gas flow field. Often the coupling between the solid and gas phases is one-way and it is usual to ignore particle to particle interactions and the volume occupied by the solid phase. For fluidized beds where there are high solids loading and strong interactions between individual particles and the gas and particle phases the particle tracking Eulerian–Lagrangian method is unsuitable. An alternative Eulerian–Lagrangian method is to use the discrete element method (DEM) for the solid phase with coupling to a Eulerian gas field. DEMs are able to handle particle–particle interactions and have been applied to small scale two-dimensional fluidized bed problems [6]. Limited three-dimensional simulations have also been performed, however the DEM becomes prohibitively computational expensive as the number of particles increase making it currently unsuitable for medium to large sized problems.

The Eulerian–Eulerian method uses temporal and spatial averaging of particle and fluid variables along with principles of mass, momentum and energy conservation to obtain continuum equations for each phase. Time and length scales over which the variables are averaged correspond to the time step and cell size and need to be sufficiently small that only small changes in the variables occur across them. The resulting set of equations are similar in form to the single phase Navier–Stokes equations. Details on the derivation of the continuum equations for fluidized beds are provided by Gidaspow [7]. For the present study a two-phase isothermal Eulerian–Eulerian approximation is used with the particle phase limited to a single diameter. In this model the necessary continuum equations for volume fraction and velocities are:

$$\frac{\partial(\alpha_g \rho_g)}{\partial t} + \nabla \cdot (\alpha_g \rho_g \mathbf{u}_g) = 0, \quad (1)$$

$$\frac{\partial(\alpha_s \rho_s)}{\partial t} + \nabla \cdot (\alpha_s \rho_s \mathbf{u}_s) = 0, \quad (2)$$

$$\frac{\partial(\alpha_g \rho_g \mathbf{u}_g)}{\partial t} + \nabla \cdot (\alpha_g \rho_g \mathbf{u}_g \mathbf{u}_g) - \nabla \cdot \left\{ \alpha \mu \left[\nabla \mathbf{u} + (\nabla \mathbf{u})^T \right] \right\}_g = -\alpha_g \nabla p + \beta (\mathbf{u}_s - \mathbf{u}_g) + \alpha_g \rho_g \mathbf{g}, \quad (3)$$

$$\frac{\partial(\alpha_s \rho_s \mathbf{u}_s)}{\partial t} + \nabla \cdot (\alpha_s \rho_s \mathbf{u}_s \mathbf{u}_s) - \nabla \cdot \left\{ \alpha \mu \left[\nabla \mathbf{u} + (\nabla \mathbf{u})^T \right] \right\}_s = -\alpha_s \nabla p + \beta (\mathbf{u}_g - \mathbf{u}_s) + \alpha_s \rho_s \mathbf{g} - \nabla p_s, \quad (4)$$

where α is volume fraction, ρ the material density, \mathbf{u} the velocity vector, p pressure, p_s the solid pressure, μ the dynamic viscosity, β the interphase momentum transfer coefficient, \mathbf{g} the gravity vector, g indicates the gas phase and s the solids phase.

2.2. Constitutive equations

To close the above equation set constitutive equations that are required for the interphase momentum transfer coefficient and the solid pressure terms [4]. The interphase momentum transfer coefficient, in regions where the gas volume fraction is less than 0.8, can be approximated as:

$$\beta = 150 \frac{(1 - \alpha_g)^2 \mu_g}{\alpha_g (\phi d_p)^2} + 1.75 \frac{\rho_g |\mathbf{u}_g - \mathbf{u}_s| (1 - \alpha_g)}{\phi d_p}, \quad (5)$$

where d_p is particle diameter and ϕ being the particle sphericity factor. Eq. (5) is derived from the well known Ergun equation [8] widely used for predicting pressure drop in fluidized beds. In regions of lower particle concentrations the interphase momentum transfer coefficient is obtained from a modified form [9,10] of the single particle drag correlation and is given by:

$$\beta_g = \frac{3}{4} C_d \frac{\alpha_g \rho_g |\mathbf{u}_g - \mathbf{u}_s| (1 - \alpha_g)}{\phi d_p} \alpha_g^{-2.65}, \quad (6)$$

$$C_d = \begin{cases} 24 \frac{(1 + 0.15 \text{Re}^{0.687})}{\text{Re}} & \text{Re} \leq 1000, \\ 0.44 & \text{Re} > 1000 \end{cases} \quad (7)$$

with Re being the particle Reynolds number given as:

$$\text{Re} = \frac{\rho_g |\mathbf{u}_s - \mathbf{u}_g| \alpha_g \phi d_p}{\mu_g}. \quad (8)$$

Relative motion of particles and collisions with adjacent particles gives rise to shear and normal forces between particles. Following the single-phase convention, these forces are referred to as a solids stress with the normal stress component known as solids pressure. Applying the kinetic theory of dense gases to solid particles recent workers [3,11] have developed a kinetic theory model for predicting these stress components by solving an additional equation for solids temperature. Only limited results have been obtained using this model and questions still exist regarding constitutive relationships in the model. In the current work a fixed viscosity value is used for the shear stress term. To model the contact force occurring between particles that prevents particle packing beyond their maximum packing fraction, a solid phase pressure term is added to the solid phase momentum equations and is taken to be:

$$\nabla p_s = -e^{-c(\alpha_g - \alpha^*)} \nabla \alpha_g, \quad (9)$$

where values [4] for the constants c and α^* are 100 and 0.45, respectively.

2.3. Numerical solution technique

Solution of Eqs. (1)–(4) is achieved using a finite volume method on a collocated grid. A segregated iterative procedure is used to solve the equations where for each iteration the velocity equations are solved, followed by a pressure correction step where a single equation is derived using an extended form of the SIMPLE technique to adjust the velocities so that global mass conservation is maintained. Finally the volume fraction equations are solved to update the individual phase volume fractions based on phase mass conservation and the requirement that they sum to unity. Thus for each iteration five equations are solved. Typically between 10 and 20

iterations are required at each time step to reduce the global mass continuity error to 0.1% of the inlet gas mass flow rate.

Strong coupling between the phases requires that the interphase transfer terms be handled using a semi-implicit method to aid convergence. In the present model this is achieved using a method similar to the Inter Phase Slip Algorithm of Spalding [12]. The computational engine used for solving the equations is the commercial finite volume program, CFX [3]. Interphase transfer and solid pressure terms are added into CFX via a User FORTRAN interface.

3. Three dimensional bubble formation

3.1. Model description

To demonstrate the capability of the model the problem of a bubbling three-dimensional fluidized bed riser is studied. Riser geometry and operating conditions are based on a physical model being used to study the isothermal hydrodynamics of a Winkler style gasifier. Geometry of the riser consists of a vertical 300 mm diameter cylinder of length 3 m sitting on top of a 800 mm long conical section as shown in Fig. 1. Fluidizing air at atmospheric conditions enters the conical section of the model at two levels. At each level, three nozzles, uniformly distributed around the circumference, feed air into the conical section. To prevent solid material building up in the base of the cone a small quantity of air with a velocity of 0.1 m/s enters through the base of the cone. Air supplied to the riser through the inlets is set to give a mass flow rate of 198.7 kg/h which corresponds to a superficial riser velocity of 0.58 m/s. A constant pressure boundary is used at the top of the riser. Non-slip walls are used for both the gas and solid phases.

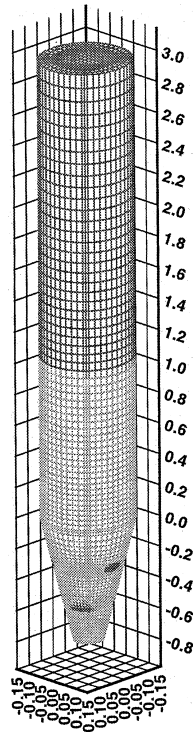


Fig. 1. Riser mesh (fine grid model).

In the original physical modelling work cork was used as the solid material and is used in this work for the solid particles with a density of 282 kg/m^3 , a particle diameter of 1.1 mm and a sphericity factor of 0.69. To account for viscous effects in the particle phase a value of 1.0 Pa/s for the solid phase viscosity is used, based on published values [4,13] for sand in bubbling and circulating fluidized beds as values for cork were not available. The fluidizing gas is assumed to be air at atmospheric conditions. Initially the riser is partly filled with solid material with a volume fraction of 0.53 giving a total solids inventory of 14.48 kg. A time step of 0.001 s is used for the simulation.

To avoid numerical problems arising from non-orthogonal cells and problems arising from the use of an axis of symmetry, a “five-block” pipe grid is used. The block arrangement is achieved using body fitted coordinates as shown by the horizontal plane in Fig. 2. A central near rectangular block is surrounded by four outer blocks, each of which form a radially truncated segment.

Grid sensitivity of the calculation is assessed by performing two calculations with different numbers of cells. For the coarse mesh calculation six cells are used circumferentially for each of the four outer blocks. For cells to match at block boundaries this requires the central block to have six by six cells. For the outer blocks two cells are used in the radial direction. In the vertical direction the cone has 18 cells and the parallel section of the riser has 50 cells.

In the fine mesh calculation the number of cells in each segment is doubled to 12 while the number of radial cells in the four outer blocks is increased to three. The number of vertical cells for the cone and riser are 55 and 36, respectively giving a total of 26 208 cells. In the coarse mesh calculation a total of 5712 cells are used. Approximate CPU time for half a second of real time is 25 h for the coarse mesh model on a 55 MHz SUN SPARC 10 and 55 h for the fine mesh calculation on a 90 MHz SUN SPARC 10.

For both calculations the grid is refined in the vertical direction to concentrate cells in the bed region. It is not possible to accurately represent the circular nature of the gas inlets. For the coarse mesh calculation each inlet is represented by an individual cell approximately rectangular in shape and normal to the gas flow. Cross sectional area of the cell face is equal to that of the actual inlet tube to give the correct mass and momentum sources into the model. For the fine mesh calcu-

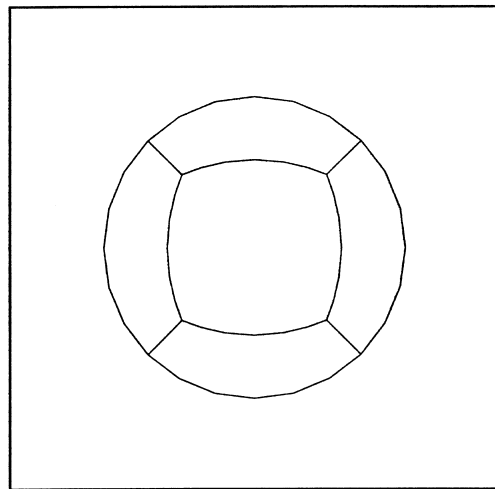


Fig. 2. Radial block configuration in riser showing “five block” pipe arrangement.

lation each inlet consists of four cells also approximately rectangular in shape and of equal area to the inlet tubes.

3.2. Results

Results obtained for 2 s of real time for the coarse and fine mesh model are presented in the form of gas phase iso-contours in Figs. 3–5. The iso-contours are at a gas phase volume fraction of 0.8 which in two-dimensional visualisation studies [2] has been found to have indicated the boundary of bubbles. Figs. 6 and 7 are from the fine mesh calculation and show contours of solids volume fraction, at 0.1 intervals, on twelve horizontal planes at various heights for real times of 1.2 and 2 s. Figs. 6 and 7 also include solids velocity vectors and volume fraction contours on a

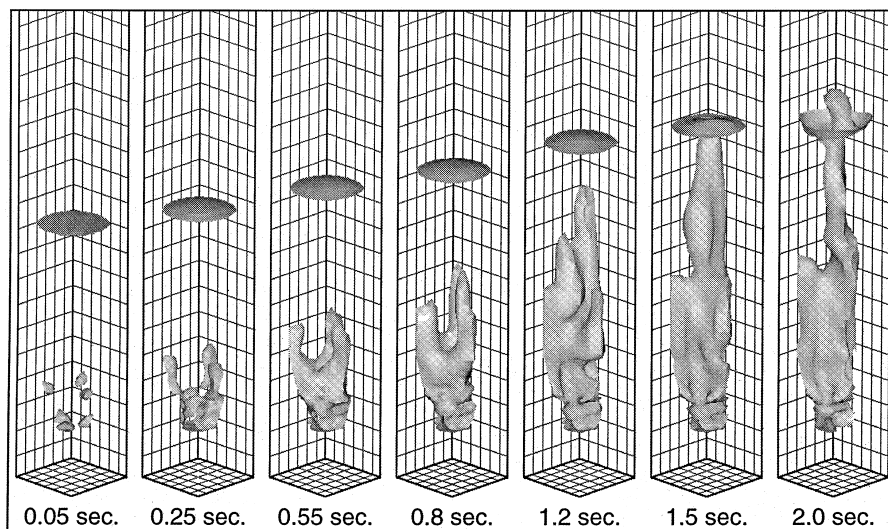


Fig. 3. Iso-contours showing bubble formation between 0.05 and 2.0 s with a coarse mesh (0.8 gas volume fraction).

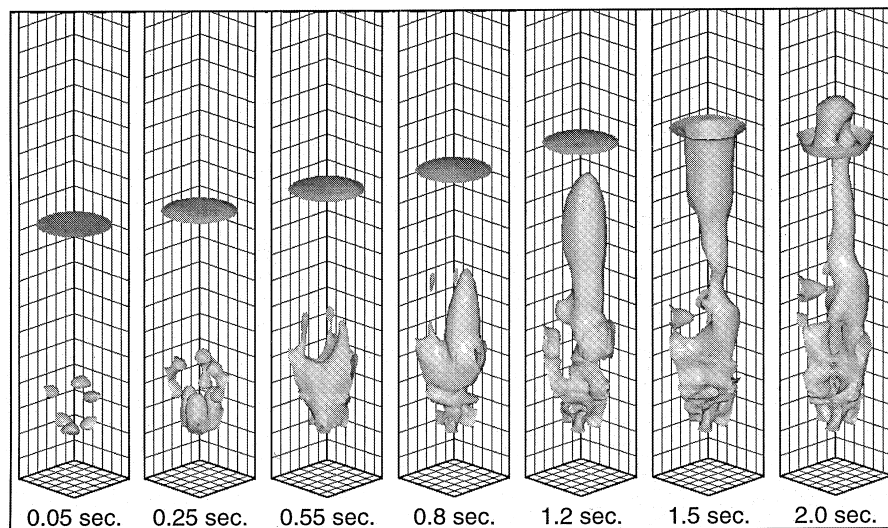


Fig. 4. Iso-contours showing bubble formation between 0.05 and 2.0 s with a fine mesh (0.8 gas volume fraction).

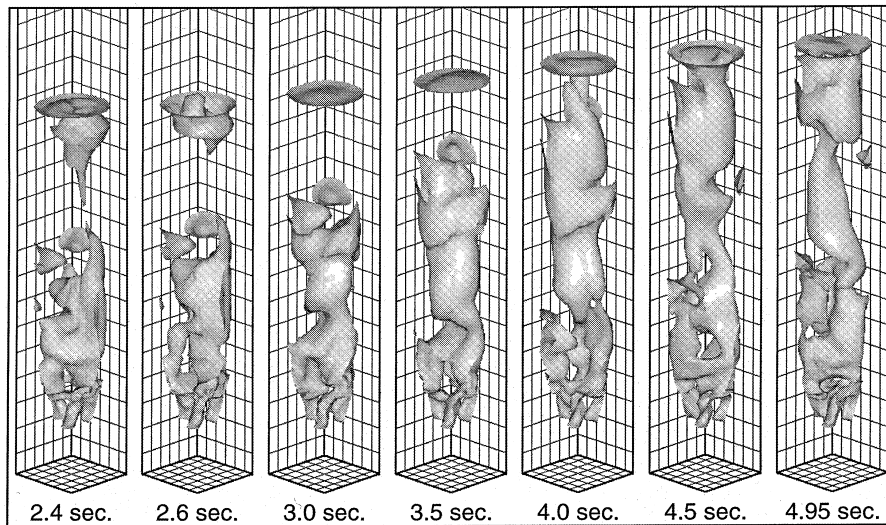


Fig. 5. Iso-contours showing bubble formation between 2.4 and 4.95 s with a fine mesh (0.8 gas volume fraction).

vertical plane at the same time instants. For visualisation purposes the vertical dimension is scaled by a factor of one-half relative to the horizontal dimensions.

At 0.05 s in Figs. 3 and 4, the locations of the six gas jets are visible as small bubbles. The bed surface appears elliptical in shape due to the three-dimensional perspective view and with time is seen to rise upward as gas enters the bed. By 0.8 s the six air jets have coalesced into a long single void which travels upward and breaks through the bed surface at about 1.3 s. Gas in the void starts leaving the bed at about 1.5 s. By 2.0 s the initial void has left the bed but solid material entrained in its wake is seen to be carried into the freeboard region. Further calculation predicts the formation of long central voids similar to the initial void and are shown in Fig. 5 for the fine mesh calculation. A few small voids are predicted to occur near the walls, but most gas travels through the central region. Such a prediction suggests that experimental techniques based solely on inspection of the outside of clear walled systems will be of limited use for gaining an understanding of gas and solid behaviour within such systems.

Fine mesh results in Fig. 4, when compared to coarse mesh results in Fig. 3, show that refining the grid has a small effect on the solution and hence the solution is not fully grid independent. However the main features of the flow are captured in both models with the fine mesh model showing sharper bubble definition and earlier coalescence of the air jets into a single central gas void. Expansion of the bed surface, the bubble breaking through the bed surface and the solid entrainment in the wake region are all consistently predicted by both models.

Recently [14] a capacitance tomographic imaging system was used to study solids behaviour in a fluidized bed with a similar physical geometry and gas inlet system to that of the present model. Transient radial gas voidage distributions were obtained at a location 640 mm above the junction of the cone and the riser. Material and thus operating conditions vary from the current model and thus prevent a quantitative comparison, however qualitatively the results support the model predictions. At air velocities near the minimum fluidization velocity an almost uniform distribution was observed experimentally with occasional gas voids. At higher gas velocities long central gas voids form surrounded by solids near the walls at the minimum fluidization voidage. Between gas voids the solids concentration in the centre of the riser increases but remains substantially below the minimum fluidization volume fraction near the walls. Such behaviour is

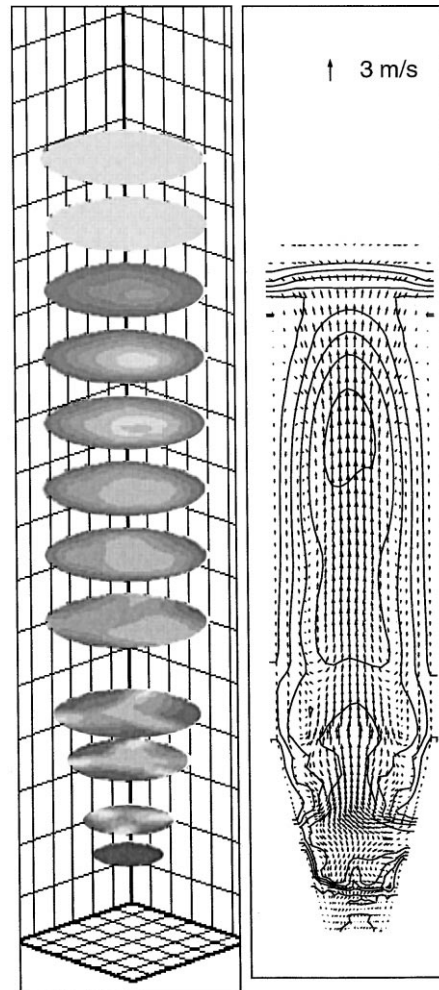


Fig. 6. Plots of volume fraction and solids velocity vectors at 1.2 s.

qualitatively consistent with predictions of the current model. This behaviour is evident that the volume fraction plots in Figs. 6 and 7.

Velocity vectors in Fig. 6 show the upflow of solid material in the bubble region with solids velocities in the order of 3 m/s. Near the walls the solids are predicted to flow downward with a velocity of approximately 0.5 m/s. Flow of solids in the bubble wake region indicates the entrainment of solids from the wall region into the centre of the fluid bed indicating one of the mixing mechanisms in fluidized beds. The complex flow in the cone section arises from the air jets which are out of plane. Effect of the air jets on the solids is more clearly shown in Fig. 7 where the plane is through two of the air jets. Fig. 7 is at 2.0 s of real time and the gas voids have become asymmetrical. Velocities in the gas voids are typically 3 m/s whilst near the wall the solids move downward at 0.2–0.5 m/s. The volume fraction contours indicate that there is a gradual transition rather than a sharp interface between the voids and solids. Observations from physical models indicate that this interface should be reasonably sharp suggesting smearing due to numerical diffusion. Other work [15,16] indicates that higher order differencing schemes can sharpen the interface at the cost of additional CPU time.

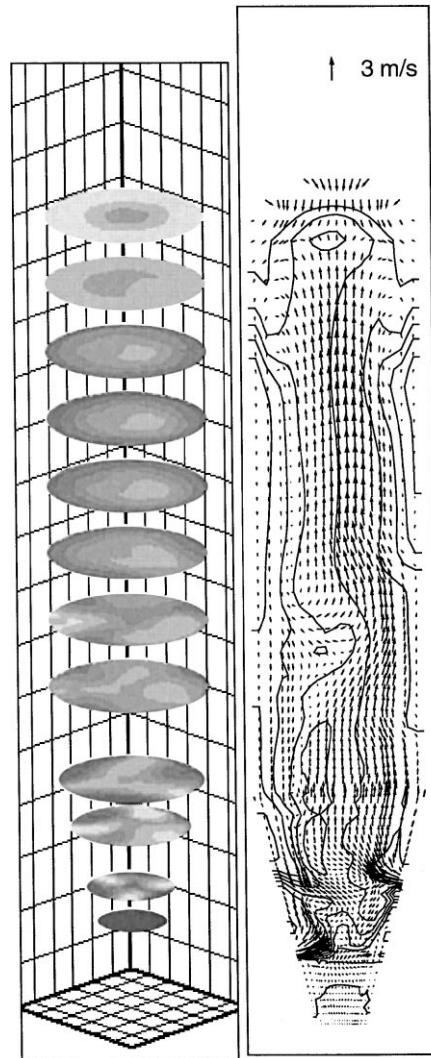


Fig. 7. Plots of volume fraction and solids velocity vectors at 2 s.

4. Conclusions

A transient three-dimensional multiphase fluidized bed model has been developed using the commercial CFD code, CFX, as the computational engine. Close coupling between the two phases requires the use of small time steps and consequently large CPU time requirements.

Results presented in this paper show that CFD technique is capable of predicting typical behaviour such as bubble formation and motion observed in a complex fluidized bed system.

A lack of detailed experimental data combined with the large CPU time requirements prevent quantitative validation of model predictions at this time. Model results show that advanced experimental techniques are needed to obtain experimental data for model validation. Recent experimental results are in reasonable qualitative agreement with predictions of the model. Further work to improve confidence in the CFD model predictions of complex multiphase systems is required. Such work would include collection of validation data, improvements to physical models for the hydrodynamics and means of reducing CPU time requirements of the model.

Acknowledgements

Code to enable modelling of bubble formation in a 3D fluidised bed has been licenced to AEA Technology and incorporated in the latest version of CFX4. The authors acknowledge the agreement of AEA Technology to publish this work. The authors wish to acknowledge the financial and other support received for this research by the Cooperative Research Centre for New Technologies for Power Generation from Low Rank Coal, which is established and supported under the Australian Government's Cooperative Research Centres program.

References

- [1] J.X. Bouillard, R.W. Lyczkowski, Hydrodynamics/heat-transfer/erosion predictions for a cold small-scale CFBC, in: *Proceedings of the Fourth International Conference on Circulating Fluidized Beds, Preprint Volume, 1993*, pp. 442–447.
- [2] L.X. Bouillard, R.W. Lyczkowski, D. Gidaspow, Porosity distribution in a fluidized bed with an immersed obstacle, *AIChE J.* 35 (1989) 908–922.
- [3] J. Ding, D. Gidaspow, A bubbling fluidization model using kinetic theory of granular flow, *AIChE J.* 36 (1990) 523–538.
- [4] J.A.M. Kuipers, W. Prins, P.M. van Swaaij, Theoretical and experimental bubble formation at a single orifice in a two-dimensional gas-fluidized bed, *Chem. Eng. Sci.* 46 (1991) 2881–2894.
- [5] CFDS, CFDS-FLOW3D Release 3.3 User manual, Computational Fluid Dynamics Services, AEA Industrial Technology, Harwell Laboratory, Didcot, Oxon, UK, 1993.
- [6] Y. Tsuji, T. Kawaguchi, T. Tanaka, Discrete particle simulation of two-dimensional fluidized bed, *Powder Tech.* 77 (1993) 79–87.
- [7] D. Gidaspow, *Multiphase Flow and Fluidization*, Academic Press, New York, 1994.
- [8] S. Ergun, Fluid flow through packed columns, *Chem. Eng. Prog.* 48 (1952) 89–94.
- [9] J.F. Richardson, W.N. Zaki, Sedimentation and fluidization: Part 1, *Trans. Inst. Chem. Eng.* 32 (1954) 35–53.
- [10] C.Y. Wen, Y.H. Yu, Mechanics of fluidization, *Chem. Eng. Prog. Symp.* 62 (1966) 100–111.
- [11] J.T. Jenkins, S.B. Savage, A theory for the rapid flow of identical, smooth, nearly elastic spherical particles, *J. Fluid Mech.* 130 (1983) 187–202.
- [12] D.B. Spalding, Numerical computation of multiphase flow and heat transfer, *Recent Advances in Numerical Methods in Fluid Mechanics*, in: C. Taylor, K. Morgan (Eds.), Pineridge, Swansea, 1980, pp. 139–168.
- [13] A. Miller, D. Gidaspow, Dense, vertical gas–solid flow in a pipe, *AIChE J.* 38 (1992) 1801–1815.
- [14] B.J. Mathers, M.J. Rhodes, Use of process tomography to study the structure of a gas–solid fluidized bed, in: *Proceedings of Chemeca 96, vol. 5, Sydney, 30 September – 2 October 1996*, pp. 57–62.
- [15] D.F. Fletcher, P.J. Witt, Numerical studies of multi-phase mixing with application to some small-scale experiments, *Nucl. Eng. Design* 166 (1996) 135–145.
- [16] P.J. Witt, J.H. Perry, A study in multi-phase modelling of fluidized beds, *Computational Techniques and Applications, CTAC95*, in: R. May, A. Easton (Eds.), World Scientific, Singapore, 1995, pp. 787–794.